Soft Matter

Dynamic Article Links

Cite this: *Soft Matter*, 2011, **7**, 4851

www.rsc.org/softmatter

PAPER

Surface defects in polyelectrolyte multilayers: Effects of drying and deposition cycle†

Liming Wang,[a] Li Wang[b] and Zhaohui Su*[a]

Received 30th January 2011, Accepted 11th March 2011
DOI: 10.1039/c1sm05158j

Layer-by-layer deposition has been used extensively to fabricate ultrathin films, yet some fundamental aspects of this seemingly simple methodology remain unclear, such as defects and factors controlling their formation. In this work we use charged gold nanoparticles as a probe to assess charge distribution on polyelectrolyte multilayer surfaces. This straightforward approach revealed that while excess charges are present rather uniformly throughout most of the surface, there are isolated domains free of excess charges, *i.e.* surface defects. Analysis of defect size distribution indicated that the defects are formed *via* desorption of individual polyelectrolyte chains from the surface. It was further revealed that intermediate drying in between polyelectrolyte depositions can reduce surface defect by >90%, resulting in more coherent films. Area fraction of defects was found to decrease with the number of layers deposited. These surface defects result in significant contact angle hysteresis.

Introduction

Constructing films of defined composition onto solid surfaces by alternating exposure to solutions of polycations and polyanions, *i.e.* the layer-by-layer technique, has drawn much attention during the past decade, largely because of their potential applications in various fields such as nonlinear optics, electrocatalysis, water-repellent surfaces, biosensors, permeation-selective membranes, and smart coatings.[1–8] The basic feature of the persistent buildup of a polyelectrolyte multilayer (PEM) is charge reversal at the surface after each layer deposition as numerous ionic groups on the adsorbed polymer chain remain exposed into the solution, which will pair with oppositely charged groups on the molecules deposited next.[9,10] Polyelectrolyte conformation at the surface is mainly determined by their properties and adsorption conditions,[11–13] and the intermediate treatments such as washing step may lead to reconformation of the adsorbed polyelectrolytes or detachment of the loosely-attached polyelectrolytes.[14,15] For example, it has been reported that 5 min washing can even remove about 10% of a deposited polyelectrolyte layer.[16] The complexity of the deposition behavior for polyelectrolytes precludes the possibility of ideal uniform composition of the PEMs. Actually, defects, *i.e.* chemically heterogeneous domains, are always concomitant with these PEMs, and it has been shown that defects in PEMs have significant effects on their transport properties.[17,18] It has been observed that PEM surfaces can exhibit significant water contact angle hysteresis,[5,19] suggesting that defects are probably present on PEM surfaces. However, direct observation of defects in PEMs is lacking and the factors controlling their formation are not well understood.

As PEMs are prepared from adsorption processes at a solid/liquid interface, processing parameters have important effects on the buildup and structure of the PEMs, such as temperature, solution pH, ionic strength, and the drying process *etc.*[13,16,20–25] Although other parameters have been well investigated, how drying after each deposition step affects the film structure and composition is still not clear. For example, it has been reported that intermediate drying does not cause any irreversible changes in the structure of PEM made of poly(L-glutamic acid) and poly(L-lysine),[22] whereas others indicated that drying would increase the thickness of PEMs assembled from poly (sodium 4-styrene sulfonate) (PSS) and poly(allylamine hydrochloride).[16,25]

Herein, we present a simple approach to directly disclose surface defects in PEMs by using negatively charged gold nanoparticles (AuNPs) as a probe to coordinate with positive charged groups in the topmost layer of the PEM, and to investigate the effects of drying after each deposition step on the properties of the PEM and the increase of deposition cycle on the evolution of the PEM properties.

[a]*State Key Laboratory of Polymer Physics and Chemistry, Changchun Institute of Applied Chemistry, Chinese Academy of Sciences, Changchun, 130022, P. R. China. E-mail: zhsu@ciac.jl.cn; Fax: + 86-431-85262126; Tel: +86-431-85262854*

[b]*State Key Laboratory of Electroanalytical Chemistry, Changchun Institute of Applied Chemistry, Chinese Academy of Sciences, Changchun, 130022, P. R. China*

† Electronic supplementary information (ESI) available: AuNPs on $PEM_{4.5}$, UV-vis, XPS and AFM data for PEM_4, and a video clip showing water contact angle jumps. This material is available free of charge *via* the Internet. See DOI: 10.1039/c1sm05158j

This journal is © The Royal Society of Chemistry 2011

Experimental

Materials

Poly(ethyleneimine) (PEI, Mw 25 000), Poly(diallydimethylammonium chloride) (PDDA, M_W 200 000 to 350 000), poly(sodium 4-styrene sulfonate) (PSS, M_W 70 000), and sodium tetrahydroborate ($NaBH_4$) were purchased from Sigma-Aldrich and used as received. Hydrogen tetrachloroaurate ($HAuCl_4 \cdot 3H_2O$) and sodium citrate were obtained from Beijing Chemical Co. (China). Sodium perfluorooctanoate (PFO, 0.10 M) was prepared by reacting 0.010 moles of perfluorooctanoic acid ($CF_3(CF_2)_6COOH$, Aldrich) with NaOH (Sinopharm Chemical Reagent Co., Ltd) in water and the volume of the solution was increased to 100.0 mL. Water (18.2 MΩ cm) was purified with a Millipore Simplicity system and used for all the experiments.

Substrate treatment

Silicon wafers ((100) with a SiO_2 surface layer of about 200 nm thick, Wafer Works, China) were cleaned in a hot piranha solution (H_2SO_4/H_2O_2, 7 : 3 mixture) at 80 °C for 30 min and then washed sequentially with copious amounts of acetone, ethanol and water prior to use.

Preparation of Au nanoparticles (AuNPs)

Citrate stabilized AuNPs (~3 nm) were prepared following a literature procedure.[26] Briefly, 0.5 mL of 1% aqueous $HAuCl_4 \cdot 3H_2O$ was added with vigorous stirring to 50 mL water yielding a bright yellow solution, and then 0.5 mL of 1% sodium citrate solution was added 2 min later. After another 1 min, 0.5 mL of 0.075% $NaBH_4$ in 1% sodium citrate solution was added, and the solution color changed to ruby red. This was vigorously stirred for 10 min, and then stored at 4 °C prior to use. The solution pH was about 4.6.

Layer-by-layer deposition, AuNPs attachment, and surface hydrophobization

At room temperature, a clean silicon wafer was first immersed into a PEI aqueous solution (1.0 mg/mL, pH 7.0) for 15 min, and then sequentially dipped in PSS (1.0 mg/mL) and PDDA (1.0 mg/mL) aqueous solution for 15 min each for 4 or 8 cycles with 1 min water rinsing and then mild nitrogen-flow drying (until the film was completely dry, only employed in preparation of dried PEMs) in between each deposition step. Citrate stabilized AuNPs were attached onto the surfaces by immersing the PEM-coated substrates into the solution of AuNPs for 3 min, followed by rinsing with water for 1 min and drying. The surface hydrophobization was performed by immersing the PEMs into an aqueous solution (0.10 M) of PFO for 3 min, followed by rinsing with water for 1 min and nitrogen drying.

Characterization

Surface roughness of the PEMs carrying PFO counteranions and surface morphology of the PEMs coordinated with AuNPs were characterized by tapping mode atomic force microscopy (MAC III mode SPM, Agilent). Before AFM measurements, wet PEMs were dried through slow water evaporation by storing under a petri dish for 48 h with at ~30% air humidity after the assembly was complete. Transmission electron microscopy (TEM) was carried out on a JEM-2010 microscope with an accelerating voltage of 100 kV. A small piece of the PEM bearing AuNPs was peeled off from a silicon wafer in a dilute solution of hydrofluoric acid, and then transferred to carbon coated copper grids for TEM measurements. The 200 nm SiO_2 surface layer on the Si wafer ensures complete separation of the PEMs from the substrate. Water contact angle was measured using a Krüss DSA10-MK2 drop shape analyzer at room temperature using water as the probe fluid (4 μL). A water drop was made on the needle of a syringe above the sample, and the substrate was moved up slowly until the water drop contacted the sample. Advancing and receding contact angles were determined as a small amount of water was added and withdrawn from the drop, respectively. Each contact angle value reported was an average of at least five independent measurements, and the standard deviations were less than 2°. UV-vis spectra were collected on a Shimadzu UV-2450 spectrophotometer. X-ray photoelectron spectra (XPS) were obtained on a Thermo-Electron ESCALAB 250 spectrometer equipped with a focused monochromatic Al X-ray source (1486.6 eV). The spectra were recorded at a 60° takeoff angle (between the sample surface and the detector) with 20 eV pass energy.

Results and discussion

The PEMs used in this study were the typical ones. One layer of PEI was pre-assembled onto the substrate to diminish the effect of the substrate, and then PSS and PDDA were alternately deposited onto the substrate until a desired number of bilayers was reached, with PDDA as the topmost layer. Two types of PEMs were prepared. The ones assembled with N_2 drying after each deposition step are denoted PEM_n^{dry}, and the ones prepared without N_2 drying, PEM_n^{wet}, where n indicates the number of bilayers. According to previous studies,[2,20,27,28] the surface of these PEMs capped with PDDA carries abundant excess ammonium groups from the PDDA not paired with sulfonate groups of the PSS, with small counteranions that can be readily exchanged by other anionic species.[27,28]

AuNPs with a diameter of about 3 nm were used as the probe because they are much smaller than the typical size of the polycation used here.[29] The formation of the AuNPs was examined

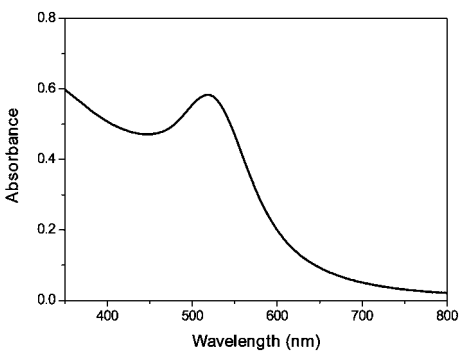

Fig. 1 UV-vis spectrum of the solution of as-prepared AuNPs.

This journal is © The Royal Society of Chemistry 2011

by UV-vis, and the spectrum is shown in Fig. 1. The strong surface plasmon band at 516 nm characteristic of monodispersed colloidal Au suggests the absence of AuNP aggregates in the solution. The AuNPs were negatively charged at pH of 4–10, a broad pH range that is convenient for our subsequent experiment. When a PEM with a PDDA cap layer is brought in contact with the AuNP solution, the negatively charged AuNPs should readily adsorb to the PEM surface *via* electrostatic interactions. This was confirmed by atomic force microscopy using PEM_4 as an example. As seen in Fig. 2, both the wet and dried PEM surfaces are densely covered by AuNPs, and there also appears no regularity of the AuNP distribution for both surfaces. The PEM surfaces before AuNP adsorption were rather flat and featureless (ESI).† The AuNPs can be observed better in the TEM images displayed in Fig. 3. First it can be seen that most of the surface is covered by the AuNPs, however, there are still many nanoscale patches with absolutely no AuNPs. As a sharp contrast, for a PEM capped with a PSS layer, the same negatively charged AuNPs were only observed on scarce number of nanoscale areas of the PEM surface, with most of the surface free of the AuNPs (Fig. S2, ESI).† These results, together with our previous findings on counterion exchange at PEM surfaces,[27,28] clearly indicate that the negatively charged AuNPs adsorb to PEM surfaces *via* electrostatic interactions, and thus can visualize and represent the distribution of the excess positive charges (PDDA units not paired with PSS units) on the surface. More specifically, the presence of AuNPs indicates that the area is rich in free PDDA units, whereas the isolated nanoscale patches where the negatively charged AuNPs cannot be attached through electrostatic interactions are absent of free cationic groups, corresponding to the surface defects.

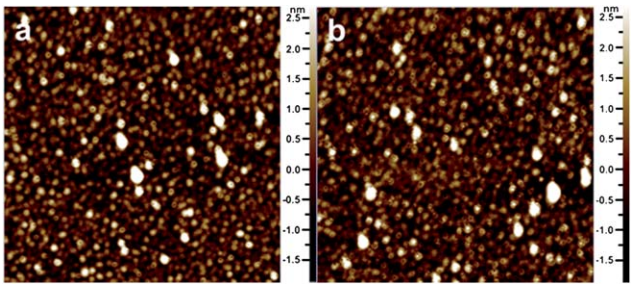

Fig. 2 AFM images of PEM_4^{wet} (a) and PEM_4^{dry} (b) after coordination with AuNPs. Images are 1 μm × 1 μm, and the z scales are as shown.

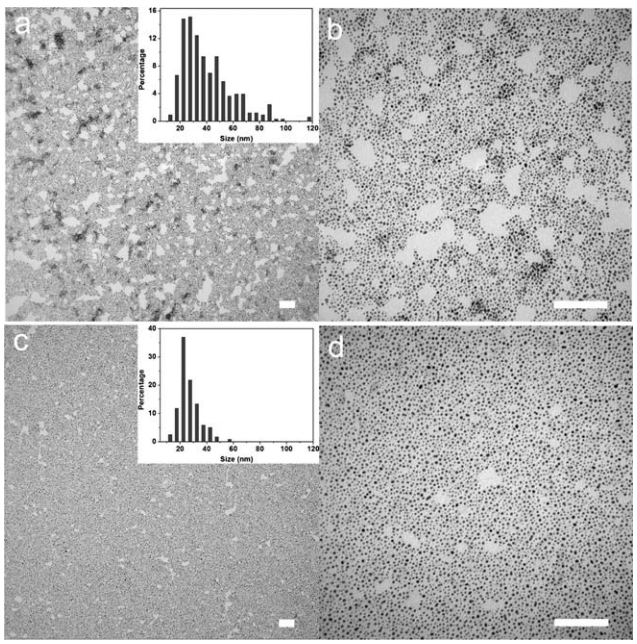

Fig. 3 TEM images of PEM_4^{wet} (a and b) and PEM_4^{dry} (c and d) coordinated with AuNPs. The insets are size distribution of the defects. The scale bars are 100 nm.

More information can be extracted from these TEM images. It can be observed that much more and larger defects are randomly located on the surface of PEM_4^{wet} (Fig. 3a, b) than PEM_4^{dry} (Fig. 3c, d). More than 40% of the defects on PEM_4^{wet} were larger than 40 nm (Fig. 3a, inset). In sharp contrast, PEM_4^{dry} had defects with a much narrower size distribution, with more than 92% falling in the range of 10 to 40 nm (Fig. 3c, inset). However, we note that in both cases the most probable defect size was ~25 nm. This is consistent with the size of a PDDA chain in solution of the molecular weight used for the assembly.[29] This suggests that the defects are formed by desorption of individual PDDA molecules from the surface. When PDDA chains adsorb to the negatively charged surface (PSS), multiple chains adsorb simultaneously and rapidly rather than negotiate with each other to have an ordered and efficient packing state (*i.e.* multilayers are not in thermodynamic equilibrium state). Therefore, while most of them adsorb with many or all charges paired (*i.e.* forming electrostatic bonds) with the PSS, the PDDA molecules approaching the now largely occupied surface have to settle in smaller footprint spaces (areas with free negatively charged PSS units) left by neighboring adsorbed chains, taking mushroom- or even brush-like conformations, with much fewer electrostatic bonds with the PSS. These PDDA chains do not stick to the surface with enough electrostatic interactions and thus are much easier to detach from the surface upon perturbation, such as rinse or immersion in another solution next, resulting in the defects observed. Furthermore, the area fraction of the defects for PEM_4^{wet} was about 19.0%, while it was only 1.7% for PEM_4^{dry}, with a ratio of greater than 11 : 1 (Table 1). These results clearly show that blow drying after each polyelectrolyte deposition in the assembly process decreases defect area prominently, leading to much more coherent PEMs.

In addition to the distinct difference in area fraction of defects, it can also be seen in Fig. 3 that there are many coil-like aggregates of AuNPs on the surface of PEM_4^{wet}, whereas the AuNPs

Table 1 Defect area fraction and water contact angles of PEMs

	Defect area fraction[a]	θ_a	θ_r	$\Delta\theta$	Surface roughness [nm][b]
PEM_4^{wet}	19.0%	61°	15°	46°	0.62
PEM_4^{dry}	1.7%	94°	12°	82°	0.87
PEM_8^{wet}	10.6%	87°	12°	75°	0.93
PEM_8^{dry}	0.9%	112°	20°	92°	0.94

[a] PEMs coordinated with AuNPs; values were obtained from two different TEM images (2 × 2 μm). [b] Root mean square value.

are distributed uniformly in the area they cover for PEM_4^{dry}. Probably when a polyelectrolyte chain adsorbs to the liquid/solid interface, it can retain some degrees of freedom by forming loops and tails into solution,[30] and further drying process then drives the loops and tails to compensate with the oppositely charged polymer by increasing hydrophobic interactions as the water content decreases. Thus drying not only decreases the amount of defects but also leads to more uniform dispersion of excess charges. Consequently more polyelectrolyte can be deposited in each cycle with intermediate drying.[25,31] This was confirmed by UV-vis and XPS data for our system. Fig. 4 compares the UV-vis spectra of PEM_4^{wet} and PEM_4^{dry}. The peak at ~225 nm is attributed to phenyl ring absorption of the PSS and can be used to quantify the PSS content in the PEM. It can be seen that more PSS has been assembled into the PEM^{dry}, and in fact the ratio of the PSS between the PEM_4^{wet} and PEM_4^{dry} was ~1 : 1.2 (Fig. 4). A same ratio was also derived from XPS data (ESI).† Moreover, similar effects were observed for the PEM_4 assembled in the presence of 0.1 M salt (ESI).†

It has been reported that buildup mechanism and properties of PEMs could vary with the number of layers assembled,[10,32–34] and thus it is of interest to investigate how the surface defects change when the number of layers assembled is increased. Fig. 5 shows the distribution of AuNPs on the surface of PEM_8. It is obvious that defects were also present on the surface of both wet and dried PEMs, and similarly, PEM_8^{wet} was far more inhomogeneous than PEM_8^{dry}, with the defect area in the former nearly 12 times that in the latter (Table 1). The size of the defects for PEM_8^{dry} appeared similar visually to that for PEM_4^{dry}; however, the size distribution is not given due to the small number of the defects on the surface. Meanwhile, the defect size distribution for PEM_8^{wet} is narrower than that for PEM_4^{wet}, with about 70% falling in the range of 10 to 40 nm in size, but the most probable size is still ~25 nm (Fig. 5a, inset), further supporting our above argument that the defects are formed *via* desorption of individual PDDA chains. Again, no apparent AuNP aggregate was observed on the surface of PEM_8^{dry}, unlike the case on the surface of PEM_8^{wet}. Furthermore, compared to PEM_4, the defect area fraction for PEM_8 was reduced by about half after 4 more bilayers were deposited. The decrease of the defect area fraction as the deposition cycle increased from 4 to 8 indicates that most of the surface defects were formed in the early stage of the assembly process, and some defects at the surface may be patched up either partially or completely upon subsequent deposition of polyelectrolyte chains.

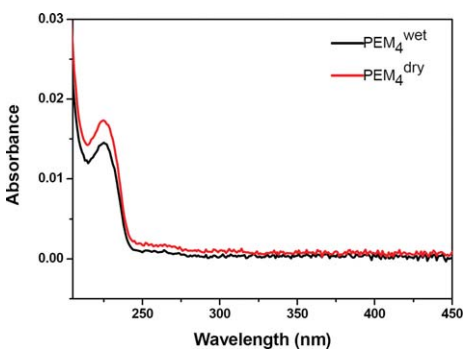

Fig. 4 UV-vis spectra of PEM_4^{wet} and PEM_4^{dry} films deposited on quartz slides.

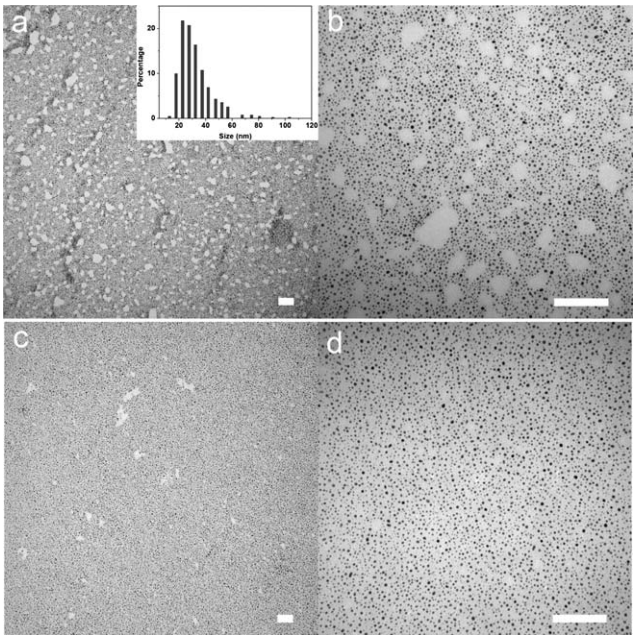

Fig. 5 TEM images of PEM_8^{wet} (a and b) and PEM_8^{dry} (c and d) coordinated with AuNPs. The inset shows the defect size distribution. The scale bars are 100 nm.

Contact angle measurement of a liquid on a solid surface is a convenient and sensitive method to characterize surface properties. Defects and roughness usually lead to contact angle hysteresis ($\Delta\theta$),[35–39] which equals to the difference between advancing (θ_a) and receding (θ_r) contact angles and has become an important criterion in judging hydrophobicity.[36] Replacing the Cl^- counterions of the excess PDDA units in the cap layer with much more hydrophobic PFO anions[27] differentiates them from the defects prominently in polarity. The defects carry no excess PDDA/PFO units and thus are still very hydrophilic. This should result in contact angle hysteresis. The surface roughness data in Table 1 show that the root mean square values of the PEMs are less than 1.0 nm, indicating that the as-prepared PEMs were flat and featureless. In this case, the effect of the defects on the hysteresis can be examined independently. It can be seen in Table 1 that θ_r is very low due to pinning of the contact line of the receding droplet by the hydrophilic defects, and are essentially the same for all PEM surfaces. The area fraction of the hydrophilic defects affects θ_a much more significantly than θ_r. The PEM_4^{wet} surface that has the largest defect area exhibits the lowest θ_a of 61°, while PEM_8^{dry} with the lowest defect area fraction shows the highest θ_a of 112°. It is clear that the smaller the defect area on the PEM surface, the higher the θ_a of the surface. These results are reasonable as a receding liquid preferentially samples high surface energy components, while an advancing liquid samples low surface energy components.[39] Consequently, $\Delta\theta$ increases from about 46° to a high value of about 92° as the fraction of surface defects decreases. Meanwhile, the strong association between the chemical defects and the water droplet induces the pinning-depinning phenomenon of the contact line[40,41] on the PEM surfaces, and distinct contact line

This journal is © The Royal Society of Chemistry 2011

jumps can be clearly observed when a water droplet advances on these surfaces (ESI).† These data demonstrate that these randomly distributed defects can have a great influence on the surface wetting properties.

Conclusions

In conclusion, we have demonstrated directly charge distribution at PEM surfaces by coordination with AuNPs, and revealed surface defects of PEMs at the molecular level. By this method, we showed that N_2 drying in between polyelectrolyte deposition steps leads to more coherent PEMs with much less surface defects than the ones without drying, and the area fraction of defects decreases with the increase of the deposition cycles. The surface defects probably are formed *via* desorption of individual polyelectrolyte chains from the surface. The PEM surfaces can exhibit high contact angle hysteresis because of the presence of randomly distributed defects. This work provides a simple but powerful way to assess the surface structure and properties of PEMs.

Acknowledgements

Z.S thanks the NSFC Fund for Creative Research Groups (50921062) for support.

Notes and references

1 G. Decher and J. D. Hong, *Makromol. Chem., Macromol. Symp.*, 1991, **46**, 321.
2 J. B. Schlenoff, H. Ly and M. Li, *J. Am. Chem. Soc.*, 1998, **120**, 7626.
3 G. Decher and J. B. Schlenoff, *Multilayer Thin Films: Sequential Assembly of Nanocomposite Materials*, Wiley, New York, 2003.
4 L. Zhai, F. C. Cebeci, R. E. Cohen and M. F. Rubner, *Nano Lett.*, 2004, **4**, 1349.
5 R. M. Jisr, H. H. Rmaile and J. B. Schlenoff, *Angew. Chem., Int. Ed.*, 2005, **44**, 782.
6 X. Zhang, H. Chen and H. Y. Zhang, *Chem. Commun.*, 2007, 1395.
7 G. Decher, *Science*, 1997, **277**, 1232.
8 J. B. Schlenoff, *Langmuir*, 2009, **25**, 14007.
9 G. Decher, J. D. Hong and J. Schmitt, *Thin Solid Films*, 1992, **210**, 831.
10 J. B. Schlenoff and S. T. Dubas, *Macromolecules*, 2001, **34**, 592.
11 A. Delcorte, P. Bertrand, E. Wischerhoff and A. Laschewsky, *Langmuir*, 1997, **13**, 5125.
12 S. S. Shiratori and M. F. Rubner, *Macromolecules*, 2000, **33**, 4213.
13 D. Yoo, S. S. Shiratori and M. F. Rubner, *Macromolecules*, 1998, **31**, 4309.
14 G. B. Sukhorukov, J. Schmitt and G. Decher, *Berichte Der Bunsen-Gesellschaft-Physical Chemistry Chemical Physics*, 1996, **100**, 948.
15 N. G. Hoogeveen, M. A. C. Stuart, G. J. Fleer and M. R. Bohmer, *Langmuir*, 1996, **12**, 3675.
16 Y. Lvov, K. Ariga, M. Onda, I. Ichinose and T. Kunitake, *Colloids Surf., A*, 1999, **146**, 337.
17 M. Chirea, V. Garcia-Morales, J. A. Manzanares, C. Pereira, R. Gulaboski and F. Silva, *J. Phys. Chem. B*, 2005, **109**, 21808.
18 Y. Wang, E. Stedronsky and S. L. Regen, *J. Am. Chem. Soc.*, 2008, **130**, 16510.
19 J. M. Levasalmi and T. J. McCarthy, *Macromolecules*, 1997, **30**, 1752.
20 S. T. Dubas and J. B. Schlenoff, *Macromolecules*, 1999, **32**, 8153.
21 R. Steitz, W. Jaeger and R. von Klitzing, *Langmuir*, 2001, **17**, 4471.
22 T. J. Halthur, P. M. Claesson and U. M. Elofsson, *J. Am. Chem. Soc.*, 2004, **126**, 17009.
23 K. Glinel, A. Moussa, A. M. Jonas and A. Laschewsky, *Langmuir*, 2002, **18**, 1408.
24 J. M. C. Lourenco, P. A. Ribeiro, A. M. B. do Rego, F. M. B. Fernandes, A. M. C. Moutinho and M. Raposo, *Langmuir*, 2004, **20**, 8103.
25 J. M. C. Lourenco, P. A. Ribeiro, A. M. B. do Rego and M. Raposo, *J. Colloid Interface Sci.*, 2007, **313**, 26.
26 G. Frens, *Nature-Physical Science*, 1973, **241**, 20.
27 L. M. Wang, Y. Lin, B. Peng and Z. H. Su, *Chem. Commun.*, 2008, 5972.
28 L. M. Wang, Y. Lin and Z. H. Su, *Soft Matter*, 2009, **5**, 2072.
29 G. Marcelo, M. P. Tarazona and E. Saiz, *Polymer*, 2005, **46**, 2584.
30 G. J. Fleer, M. A. Cohen Stuart, J. M. H. M. Scheutjens, T. Cosgrove and B. Vincent, *Polymers at Interfaces*, Chapman and Hall, London, 1993.
31 M. Raposo, R. S. Pontes, L. H. C. Mattoso and O. N. Oliveira, *Macromolecules*, 1997, **30**, 6095.
32 R. A. McAloney, M. Sinyor, V. Dudnik and M. C. Goh, *Langmuir*, 2001, **17**, 6655.
33 C. Porcel, P. Lavalle, V. Ball, G. Decher, B. Senger, J. C. Voegel and P. Schaaf, *Langmuir*, 2006, **22**, 4376.
34 C. Porcel, P. Lavalle, G. Decher, B. Senger, J. C. Voegel and P. Schaaf, *Langmuir*, 2007, **23**, 1898.
35 C. D. Bain, E. B. Troughton, Y. T. Tao, J. Evall, G. M. Whitesides and R. G. Nuzzo, *J. Am. Chem. Soc.*, 1989, **111**, 321.
36 L. C. Gao and T. J. McCarthy, *Langmuir*, 2009, **25**, 14105.
37 F. E. Bartell and J. W. Shepard, *J. Phys. Chem.*, 1953, **57**, 211.
38 C. W. Extrand, *Langmuir*, 2002, **18**, 7991.
39 C. Priest, R. Sedev and J. Ralston, *Phys. Rev. Lett.*, 2007, **99**, 026103.
40 S. Ramos and A. Tanguy, *Eur. Phys. J. E*, 2006, **19**, 433.
41 X. Jia, J. B. McLaughlin, C. Ahmadi and K. Kontomaris, *Int. J. Mod. Phys. C*, 2007, **18**, 595.